Chromatin state switching in a polymer model with mark-conformation coupling

Kyosuke Adachi[1,2,*] and Kyogo Kawaguchi[1,3,†]

[1]*Nonequilibrium Physics of Living Matter RIKEN Hakubi Research Team, RIKEN Center for Biosystems Dynamics Research,*
2-2-3 Minatojima-minamimachi, Chuo-ku, Kobe 650-0047, Japan
[2]*RIKEN Interdisciplinary Theoretical and Mathematical Sciences Program, 2-1 Hirosawa, Wako 351-0198, Japan*
[3]*RIKEN Cluster for Pioneering Research, 2-2-3 Minatojima-minamimachi, Chuo-ku, Kobe 650-0047, Japan*

We investigate the phase transition properties of the polymer-Potts model, a chain composed of monomers with magnetic degrees of freedom, with the motivation to study the conformation and mark switching dynamics of chromatin. By the mean-field approximation, we find that the phase transition between the swollen-disordered state and the compact-ordered state is discrete; it is first order as in the long-range Potts model, but with a significantly larger jump in magnetization (i.e., mark coherence) upon the ordering transition. The results imply how small changes in epigenetic writer concentrations can lead to a macroscopic switching of the chromatin state, suggesting a simple mechanism of discrete switching observed, for instance, in cell differentiation.

Introduction. Chromatin is a large polymer composed of monomers called nucleosomes, which are histone protein complexes wrapped with DNA [1,2]. The switching of cell states is encoded in the changes in epigenetics [3] such as in the molecular and structrual changes in the chromatin. The chromatin states have been traditionally categorized into two, euchromatin and heterochromatin, which correspond to active (open) and inactive (closed) parts of the chromatin in terms of gene expression and accessibility. Consistent with this, recent chromosome conformation capture (Hi-C) experiments [4,5] have identified the existence of two major compartments in the genome. The regions within the same compartment share similar marks (i.e., chemical modifications) in the nucleosomes and tend to interact with each other more frequently than across [6]. Experiments have shown that different marks on the nucleosome induce distinct interactions due to the natural attraction and repulsion between nucleosomes [7,8], or by mediating proteins such as HP1 [9,10], and the polycomb repressive complexes [11,12].

It has also been established that cell differentiation is accompanied by a large (megabase) scale transition in the compartments as well as changes in the states of epigenetic marks [5]. The mechanism behind this switching, however, remains elusive. Previous modeling studies have assumed mark-dependent interactions between nucleosomes in order to explain the observed contact maps and three-dimensional structures of the chromatin [13,14]. Other models have considered how the interaction between the marked histones lead to bistability in the coherent epigenetic marks [15–17]. A natural question is then how the interplay of chromatin chain dynamics and the kinetics of nucleosome modifications can lead to the drastic switching of compartments observed in differentiation.

To model chromatin polymer dynamics under stochastic modifications of nucleosomes, the polymer-Potts model has been considered [18–20]. In this model, the random motion of the polymer chain is accompanied by monomer-monomer interactions that depend on the histone marks, and the histone marks can stochastically switch due to enzymatic reactions and histone turnover [21,22]. It has been numerically shown [19,23] that even for the Ising-type model, where there is essentially only two distinct states of the histone marks, there is a first-order-like transition between the swollen-disordered state, which corresponds to a loose polymer with spatially random marks, and the compact-ordered state, where the conformation is globular and the marks are coherent. This abrupt transition is likely due to the coupling between the conformation change and the epigenetic switchings, although a concrete theory is still lacking.

In this Rapid Communication, we investigate the phase transition properties of the polymer-Potts model by considering a polymer chain in continuum space with stochastic histone mark exchange. Employing the Flory-type mean-field approximation for the dynamics of the chain, we write the pseudo free energy of the generic polymer-Potts model as a function of the order parameters representing the magnetization (i.e., mark coherence) and the polymer conformation. For the Ising-type interaction, the transition between the swollen-disordered state and a compact-ordered state is first order, consistent with simulations and theories investigating mark dynamics on self-avoiding random walks [18,20]. In the general case with multiple types of marks, we find that the jump in magnetization at the transition point is always larger in the polymer-Potts model compared with the Potts-model counterpart, and also obtain a criteria for the absence of a continuous transition. We further study the switching transition upon stretching of the chain, which serves as a simple model of force-induced epigenetic modification.

Model. We consider a polymer model with Potts-like interactions between monomers. The interactions are mediated in a

---
*kyosuke.adachi@riken.jp
†kyogo.kawaguchi@riken.jp

(a)

(b)
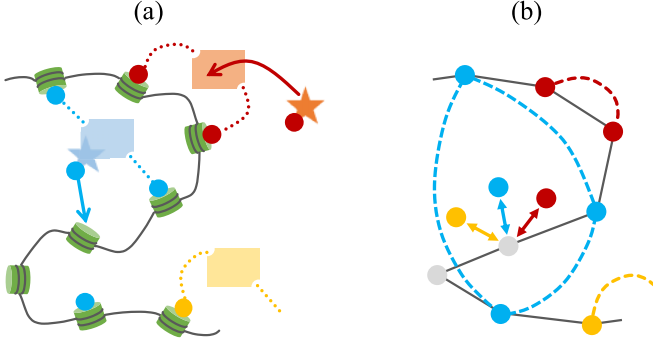
FIG. 1. (a) Chromatin consists of a DNA (gray line) wrapping histones (green cylinders). The readers (colored rectangles) connect histones with the same marks (colored circles), while the writers (colored stars) edit the histone marks. (b) The polymer-Potts model. A monomer constituting the polymer has a changeable histone mark (colored circle), and there are mark-specific interactions between monomers (colored dashed lines, J_{ij}), in addition to the mark-independent interactions (v and w).

histone-mark-dependent way by proteins that we call readers, and the marks can change stochastically due to enzymatic reactions caused by the writers (Fig. 1). We assume that there are q ($\geqslant 2$) types of marks. Extending the Flory-type mean-field approximation [24] to the present situation, the pseudo free energy (per monomer) at a temperature T reads

$$f(\rho, \{x_i\}) = v\rho + w\rho^2 - \rho \sum_{1 \leqslant i,j \leqslant q} J_{ij} x_i x_j$$
$$+ \sum_{1 \leqslant i \leqslant q} (k_B T x_i \ln x_i - h_i x_i). \quad (1)$$

Here ρ is the average monomer concentration given as $\rho \sim N/R^3$ with the polymer end-to-end distance R and the total number of monomers N. The other variables, $\{x_i\}$, represent the ith-type mark occupation ($\sum_{i=1}^{q} x_i = 1$). The first two terms in Eq. (1) correspond to the volume exclusion effect ($v, w > 0$). Note that the parameters v and w represent the second and third virial coefficients, respectively. The third term originates from the Potts-like two-body interactions between monomers mediated by the readers. The detail of the interactions between the different types of marks is coded in J_{ij}, which is a real symmetric matrix. The fourth term is the entropy associated with the mark degrees of freedom. The last term represents the effect of external fields $\{h_i\}$, which describes how much a specific epigenetic mark is favored, reflecting, for example, the concentration of the histone modification enzymes, i.e., the writers. The equilibrium state is determined by minimizing Eq. (1) with respect to ρ and $\{x_i\}$.

A few remarks are to be made for Eq. (1). Firstly, fluctuation effects are neglected compared with the microscopic model, although its inclusion will likely not change the key results [25,26]. Secondly, while higher-order interaction terms are irrelevant near the conventional second-order coil-globule transition point [24], inclusion of these terms may shift the transition point if the coil-globule transition becomes first order, as in the situations explained below. Nevertheless, we expect that Eq. (1) captures the key characters observed in simulations of similar systems [19,20] and is useful to

generally analyze models with multiple kinds of marks. Lastly, the chromatin state transition of our interest is at the level of subregions of compartments or several topologically associated domains [27], which is megabase scale corresponding to $N = 10^{3–5}$. Although we have omitted all the terms that vanish in the limit of $N \to \infty$ in Eq. (1), it is straightforward to include higher-order terms and discuss their effects on the properties of transition [24,28].

For the sake of understanding, let us first fix the mark degrees of freedom, $\{x_i\}$. Then, Eq. (1) is equivalent to the free energy of a classic polymer [24] in the large N limit. As investigated in [24], there exists a transition between the coiled state, a swollen polymer with the average length scaling as $R \sim N^{3/5}$ [29,30], and the globule state, a densely packed polymer with $R \sim N^{1/3}$ [24], upon changing the overall two-body interaction (in the present case, $v - \sum_{i,j} J_{ij} x_i x_j$) from repulsive to attractive. Such coil-globule transitions have been observed in experiments using DNA [31] and chromatin [32]. The coil-globule transition in this case is continuous in the limit of $N \to \infty$ [24], even beyond the mean-field approximation [25,26].

In another direction of simplification, we can consider the order-disorder transition of the marks under a fixed polymer density, ρ. Assuming a globular configuration ($R \sim N^{1/3}$) and $J_{ij} = J \delta_{ij}$, Eq. (1) represents the mean-field free energy of the Potts model [33]. In the limit of $N \to \infty$, the order-disorder transition is continuous for $q = 2$ while discontinuous for $q \geqslant 3$, which has been believed to be correct in three dimensions even beyond the mean-field approximation [33].

Phase transition by interactions and fields. Introducing the dimensionless globular order parameter $\phi := (w/k_B T)^{1/4} \sqrt{\rho}$, we can express the equilibrium free energy as $\bar{f} = [\min_{\phi, \{x_i\}} f(\phi, \{x_i\})$ s.t. $\sum_{i=1}^{q} x_i = 1]$, where

$$\frac{f(\phi, \{x_i\})}{k_B T} = \left(\tilde{v} - \sum_{1 \leqslant i,j \leqslant q} \tilde{J}_{ij} x_i x_j \right) \phi^2 + \phi^4$$
$$+ \sum_{1 \leqslant i \leqslant q} \left(x_i \ln x_i - \frac{h_i x_i}{k_B T} \right). \quad (2)$$

Here, the dimensionless two-body interaction strengths are defined as $\tilde{J}_{ij} := J_{ij}/\sqrt{k_B T w}$ and $\tilde{v} := v/\sqrt{k_B T w}$. As we have seen, if $\{x_i\}$ or ϕ is fixed to some value, the system described by Eq. (2) will show the conventional coil-globule or magnetic transition, respectively.

To see the effect of the coupling between $\{x_i\}$ and ϕ, we first study the Ising-model case, $q = 2$ and $J_{ij} = J(2\delta_{ij} - 1)$ with $h_i = 0$. Introducing the magnetization, $m := x_1 - x_2$, $f(\phi, m)$ for the case of $\tilde{v} = 0.1$ is shown in Fig. 2. Let us denote the equilibrium values of ϕ and m as ϕ^* and m^*, respectively. In this model, there is a critical value $\tilde{J}^{(c)}$ such that for $\tilde{J} < \tilde{J}^{(c)}$, the swollen-disordered phase is the equilibrium [$\phi^* = 0$ and $m^* = 0$; Fig. 2(a)], whereas for $\tilde{J} > \tilde{J}^{(c)}$, this switches to the compact-ordered state [$\phi^* > 0$ and $|m^*| > 0$; Fig. 2(c)]. At the transition point [$\tilde{J} = \tilde{J}^{(c)}$; see Fig. 2(b)], both the swollen-disordered state and the compact-ordered state are stable, meaning that there is a first-order transition. Thus, a switching transition can occur by simply changing the
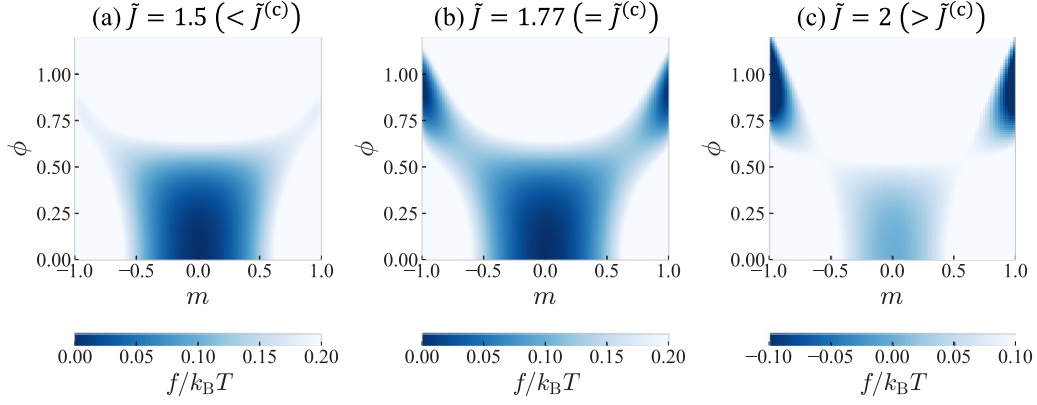
FIG. 2. Color plot of the pseudo free energy $f(\phi, m)$ [Eq. (1)] as a function of ϕ, which represents the square root of the globule density, and the magnetization m for the case of the Ising-type interaction with $\tilde{v} = 0.1$. For (a) $\tilde{J} < \tilde{J}^{(c)}$, the minimum of f is realized at $\phi = 0$ and $m = 0$ (swollen-disordered state), while for (c) $\tilde{J} > \tilde{J}^{(c)}$, it is realized at $\phi > 0$ and $|m| > 0$ (compact-ordered state). There is bistability at (b) $\tilde{J} = \tilde{J}^{(c)}$, meaning that the transition between the swollen-disordered state and the compact-ordered state is discontinuous.

strength of the reader-mediated interaction, as has been seen numerically in a similar model [19].

In Fig. 3(a) the $\tilde{J}$ dependence of ϕ^* and m^* is plotted for $\tilde{v} = 0.1$, showing a clear jump of the order parameters at the transition point. Since $|m^*| \simeq 1$ in the compact-ordered state (Fig. 2), we can approximate $\min_{\phi,m} f(\phi, m) \simeq \min_{\phi} f(\phi, m = \pm 1) = -(\tilde{J} - \tilde{v})^2 k_B T / 4$. We then obtain

$$\tilde{J}^{(c)} \simeq \tilde{v} + 2\sqrt{\ln 2}, \tag{3}$$

$$\phi^* \simeq \sqrt{(\tilde{J} - \tilde{v})/2} \quad (\text{for } \tilde{J} > \tilde{J}^{(c)}) \tag{4}$$

shown as the black dotted line in Fig. 3(a), giving a good approximation. We have confirmed that the features such as the jump of $|m^*|$ from 0 to $\simeq 1$ at the transition point are observed for a broad range of the values of $\tilde{v}$ [28].

We further consider the effect of external mark-specific fields by setting $h_1 = h$ and $h_2 = -h$ in the Ising-type model. The phase diagram in the case of $\tilde{v} = 0.1$ is shown in Fig. 3(b). We find that the field-induced transition from the swollen-disordered state to the compact-ordered state is of first order around the zero-field transition point, meaning that increasing or decreasing specific writers can also induce the switching behavior. Interestingly, within a certain range of $\tilde{J}$, sequential second- and first-order transitions occur as the field becomes stronger [Fig. 3(c)]. For a smaller $\tilde{J}$, a single continuous transition is induced by the field. Note that such a field-induced transition has been discussed in the context of the magnetic polymer within mean-field approaches [18] as well as in simulations on self-avoiding walk models [18,34].

Propeties of transitions under general settings. Here we consider the condition for the transition between the swollen and compact states to be countinuous under general q, $\{J_{ij}\}$, and $\{h_i\}$. Minimizing Eq. (2) on the assumption that the continuous transition occurs at $\{\tilde{J}_{ij}^{(c)}\}$ for a given set of $\{h_i\}$, we obtain $\phi^* = 0$ and $x_i^* = S_i(\tilde{h}) := \exp(h_i/k_B T)/\sum_{j=1}^{q} \exp(h_j/k_B T)$ [28]. The order parameters will grow in response to the deviation of the interaction strengths from their critical values: $\phi^* = \Delta\phi$ and $x_i^* = S_i(\tilde{h}) + \Delta x_i$ for $\tilde{J}_{ij} = \tilde{J}_{ij}^{(c)} + \Delta\tilde{J}_{ij}$. Minimizing Eq. (2) at $\tilde{J}_{ij} = $

$\tilde{J}_{ij}^{(c)} + \Delta\tilde{J}_{ij}$ will give the following relation:

$$2(\Delta\phi)^2 = \sum_{1 \leqslant i,j \leqslant q} \left(\tilde{J}_{ij}^{(c)} + \Delta\tilde{J}_{ij} \right)$$
$$\times [S_i(\tilde{h}) + \Delta x_i][S_j(\tilde{h}) + \Delta x_j] - \tilde{v}. \tag{5}$$

For the transition to be continuous, the order parameters should smoothly change at the transition point: $\Delta\phi \to 0$ and $\Delta x_i \to 0$ for $\Delta\tilde{J}_{ij} \to 0$, meaning that $J_{ij}^{(c)}$ should obey

$$\sum_{1 \leqslant i,j \leqslant q} J_{ij}^{(c)} S_i(\tilde{h}) S_j(\tilde{h}) = v. \tag{6}$$

Therefore, if $\sum_{i,j} J_{ij} S_i(\tilde{h}) S_j(\tilde{h}) < v$ is satisfied, which is when the mean effective two-body interaction is repulsive, any continuous swollen-compact transition is prohibited and only switchlike transitions can occur. This condition can in principle be checked in experiment by measuring the effective interactions between nucleosomes [7].

A simple example is again the Ising-type model without external fields. In this case, since $\sum_{i,j} J_{ij} S_i(\tilde{h}) S_j(\tilde{h}) = \sum_{i,j} J_{ij}/4 = 0 < v$, the continuous conformation transition is always prohibited, consistent with our numerical results that the first-order transition occurs irrespective of the value of v [28].

To investigate the order-parameter jump at the first-order transition more specifically, we consider the Potts-type interaction: $J_{ij} = J\delta_{ij}$ with $h_i = 0$. Figure 3(d) shows the magnetization jump $\Delta m = \max\{x_i^*\} - \min\{x_i^*\}$ for $q \geqslant 2$ in the mean-field polymer-Potts model [Eq. (2)] compared with the conventional mean-field Potts model. In the Potts model [33], the transition is of second order for $q = 2$ while first order for $q \geqslant 3$, and Δm is given as $(q - 2)/(q - 1)$. In the polymer-Potts model, on the other hand, the magnetic transition is always first order, and Δm is a monotonically increasing function of v and q, while the dependency on v is almost negligible for $q \geqslant 4$. Notice that Δm in the polymer-Potts model is always larger than that in the corresponding Potts model, and Δm is practically unity for $q \geqslant 4$. This suggests that the polymer conformation change that accompanies the magnetic transition reinforces the all-or-none switching property.
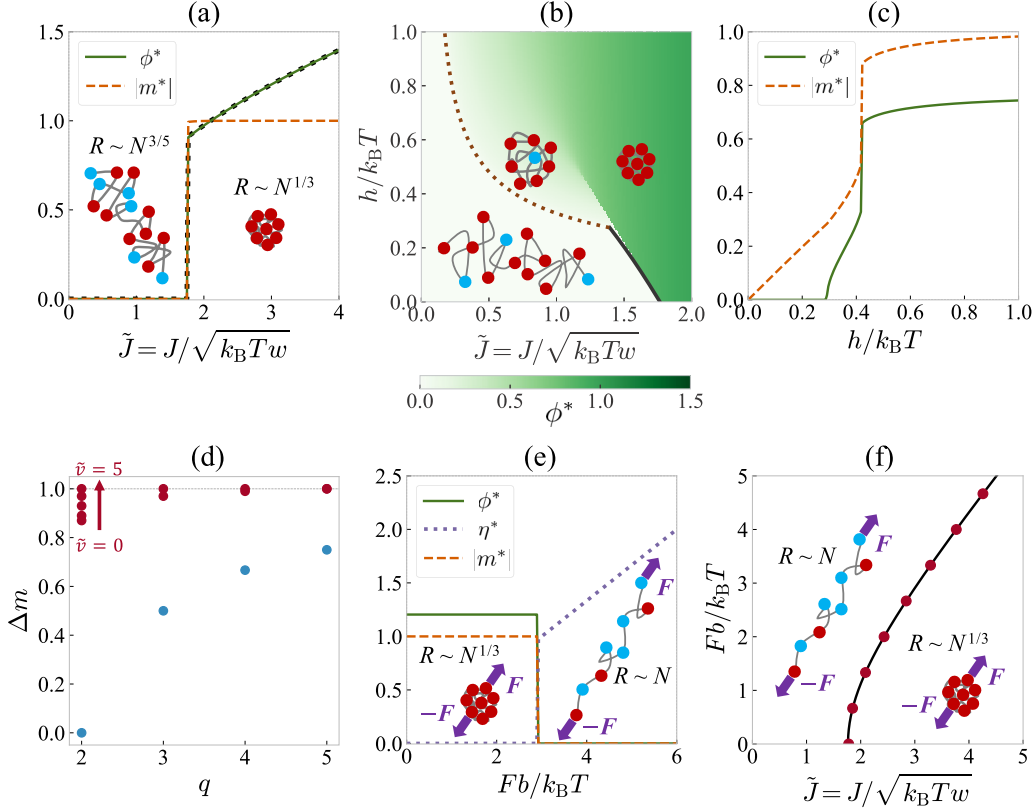
FIG. 3. (a) The globular order parameter ϕ^* (green solid line) and magnetization m^* (orange dashed line) as a function of the mark-specific interaction strength $\tilde{J}$. The approximate functional form of ϕ^* [Eq. (4)] is plotted as a black dotted line. (b) Phase diagram in the J-h plane. The analytical expressions of the second-order transition line [28] (brown dotted line) and the approximate first-order transition line [28] (black solid line) are also plotted. (c) The order parameters, ϕ^* and m^*, as a function of the external field strength h for the case of $\tilde{J} = 1.25$. (d) Magnetization jump (Δm) at the magnetic transition point as a function of the number of mark types (q) for the mean-field polymer-Potts model [red (dark-gray) points] and for the mean-field Potts model [blue (light-gray) points]. For the polymer-Potts model, Δm is plotted for several values of $\tilde{v}$ ($\tilde{v} = 0, 0.1, 0.5, 1, 5$ for $q = 2$; $\tilde{v} = 0, 5$ for $q \geqslant 3$). (e) The stretched-state order parameter η^* (purple dotted line), in addition to ϕ^* (green solid line) and m^* (orange dashed line), as a function of the external force strength F for the case of $\tilde{J} = 3$. (f) Phase diagram in the J-F plane. The small-J and large-J regions represent the stretched-disordered and compact-ordered phases, respectively. The phase boundary estimated with Eqs. (2), (7), and (8) is shown with red circles, along with the approximate $F^{(c)}(\tilde{J})$ curve [28] (black line). The transition is always of first order.

Mechanical discontinuous transition. We here consider what happens when a stretching force is applied to the edges of a polymer chain with mark degrees of freedom. For simplicity, let us investigate the effects of an external force term added to the pseudo free energy [Eq. (2)] with the Ising-type interaction. The force term can be written as $f_F = -\boldsymbol{F} \cdot \boldsymbol{R}/N$ with an external force $\boldsymbol{F}$ and the polymer end-to-end vector $\boldsymbol{R}$.

Within the mean-field level, the free energy including the effects of an external force is given as

$$\overline{f} = \min\left\{ \min_{\phi, m} f(\phi, m), \min_{\eta, m} f'(\eta, m) \right\}, \tag{7}$$

where $f'(\eta, m)$ is another pseudo free energy including the effect of the external force:

$$\frac{f'(\eta, m)}{k_B T} = -\frac{Fb\eta}{k_B T} + \frac{3}{2}\eta^2 + \frac{1+m}{2} \ln \frac{1+m}{2}$$
$$+ \frac{1-m}{2} \ln \frac{1-m}{2}. \tag{8}$$

Here, the dimensionless polymer length, $\eta := R/Nb$, can be interpreted as an order parameter characterizing a stretched

state with the scaling $R \sim N$ [35]. In Eq. (8), the second term represents the entropic elasticity [30], which is essential under stretched conditions. We denote the equilibrium point as (ϕ^*, η^*, m^*). Since the globule state ($\phi^* > 0$, $R \sim N^{1/3}$) and the stretched state ($\eta^* > 0$, $R \sim N$) are incompatible, only one of (ϕ^*, η^*) can be finite and the other should be zero.

Figure 3(e) shows the changes in order parameters upon varying of the external force F for the case of $\tilde{v} = 0.1$ and $\tilde{J} = 3$, in which the compact-ordered state ($\phi^* > 0$, $\eta^* = 0$, and $|m^*| > 0$) is stabilized when $F = 0$. We can see that a first-order transition occurs at a certain critical value $F^{(c)}$, above which a stretched-disordered state ($\phi^* = 0$, $\eta^* > 0$, and $m^* = 0$) emerges. The numerically obtained phase diagram in the J-F plane is shown in Fig. 3(f). Note that the force-induced coil-globule transitions are believed to be discontinuous also in classical polymer models at $N \rightarrow \infty$ [35–38]. In the polymer-Potts model, we find that the mark degrees of freedom become immediately disordered accompanying this stretching transition. Similar discontinuous transitions between a compact-ordered state and a stretched-disordered
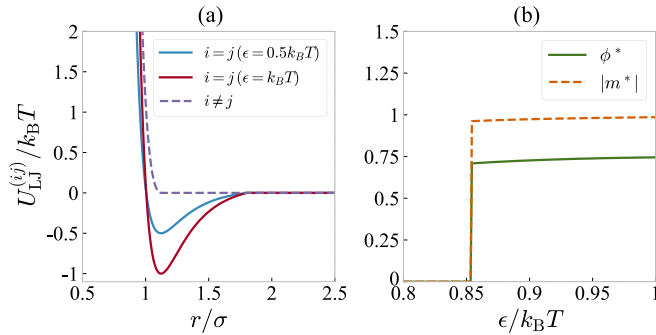
FIG. 4. (a) Lennard-Jones-type interaction $U_{\mathrm{LJ}}^{(ij)}(r)$ between two monomers ($1 \leqslant i, j \leqslant 2$). σ is the interaction length, and ϵ is the attractive interaction strength between monomers with the same mark. (b) Optimized order parameters ϕ^* and m^* as a function of the interaction strength $\epsilon/k_{\mathrm{B}}T$.

state have recently been seen in molecular dynamics simulations with short-range interactions [39].

Relation to molecular dynamics simulations. To compare our results with the molecular dynamics simulations [19] using Lennard-Jones-type interactions [Fig. 4(a)], we consider the virial expansion. By neglecting $\mathcal{O}(\phi^6)$ terms and the existence of the neutral mark, we obtain the pseudo free energy [Eq. (2)] with additional terms proportional to $m^2\phi^4$ [28].

By minimizing the pseudo free energy, we obtain the optimized ϕ^* and m^* as a function of the interaction strength $\epsilon/k_{\mathrm{B}}T$. Figure 4(b) shows that a discontinuous transition with a large jump of magnetization occurs at the interaction strength $\epsilon/k_{\mathrm{B}}T \simeq 0.85$, which is close to the simulation result [19] ($\epsilon/k_{\mathrm{B}}T \simeq 0.9$ for $N = 2000$). Although the virial expansion is not generally justfied for cases with a first-order transition, this result suggests that a simplified framework can connect the molecular level measurement of histone interactions [7] to the compartment level chromatin state transition.

Discussion and conclusion. Here we have studied the polymer-Potts model at the mean-field level and found that switchlike transitions are largely enhanced, compared with the transitions in a polymer model with unchangeable marks or the conventional Potts model, due to the coordination of the coil-globule and magnetic transition. The bistable property leading to the first-order transition fits with the phenomenology of chromatin state transition and cell differentiation. For instance, it has been shown that elimination of small kilobase-scale genome regions can induce compartment switching of a whole megabase-scale region [40]. This can be explained by the bistability of the chromatin state, which allows localized histone mark biases induced by transcription factors to spread macroscopically. The hysteresis effect, which is expected to accompany the chromatin discontinuous transition, may also improve the stability of the epigenetic regulation against chemical and mechanical perturbations and cell division.

Additional to the equilibrium phase transition scenario proposed in this Rapid Communication, nonequilibrium features of the chemical dynamics [19,20] and the phase separation properties of the key components in chromatin dynamics [8,41–44] may play roles in enhancing or diminishing the switchlike behavior. Nevertheless, the fact that a simple mark-conformation coupling can lead to a discrete switch indicates that nonlinear dynamics and well-designed chemical networks may not be essential in explaining cell fate dynamics. In real differentiation, state switching occurs in sub-regions and does not expand to the whole chromosome [5]. It is interesting to explore how specific regions in the genome set boundaries to prevent the phase transition dynamics from spreading into undesired regions [45].

[1] R. Cortini, M. Barbi, B. R. Caré, C. Lavelle, A. Lesne, J. Mozziconacci, and J.-M. Victor, Rev. Mod. Phys. **88**, 025002 (2016).

[2] B. Fierz and M. G. Poirier, Annu. Rev. Biophys. **48**, 321 (2019).

[3] C. H. Waddington, *The Strategy of the Genes: A Discussion of Some Aspects of Theoretical Biology* (Allen & Unwin, London, 1957).

[4] E. Lieberman-Aiden, N. L. van Berkum, L. Williams, M. Imakaev, T. Ragoczy, A. Telling, I. Amit, B. R. Lajoie, P. J. Sabo, M. O. Dorschner, R. Sandstrom, B. Bernstein, M. A. Bender, M. Groudine, A. Gnirke, J. Stamatoyannopoulos, L. A. Mirny, E. S. Lander, and J. Dekker, Science **326**, 289 (2009).

[5] J. R. Dixon, I. Jung, S. Selvaraj, Y. Shen, J. E. Antosiewicz-Bourget, A. Y. Lee, Z. Ye, A. Kim, N. Rajagopal, W. Xie, Y. Diao, J. Liang, H. Zhao, V. V. Lobanenkov, J. R. Ecker, J. A. Thomson, and B. Ren, Nature (London) **518**, 331 (2015).

[6] M. Di Pierro, R. R. Cheng, E. L. Aiden, P. G. Wolynes, and J. N. Onuchic, Proc. Natl. Acad. Sci. USA **114**, 12126 (2017).

[7] J. J. Funke, P. Ketterer, C. Lieleg, S. Schunter, P. Korber, and H. Dietz, Sci. Adv. **2**, e1600974 (2016).

[8] B. A. Gibson, L. K. Doolittle, L. E. Jensen, N. Gamarra, S. Redding, and M. K. Rosen, bioRxiv, 523662 (2019).

[9] A. J. Bannister, P. Zegerman, J. F. Partridge, E. A. Miska, J. O. Thomas, R. C. Allshire, and T. Kouzarides, Nature (London) **410**, 120 (2001).

[10] S. Machida, Y. Takizawa, M. Ishimaru, Y. Sugita, S. Sekine, J.-i. Nakayama, M. Wolf, and H. Kurumizaka, Mol. Cell **69**, 385 (2018).

[11] A. Angel, J. Song, C. Dean, and M. Howard, Nature (London) **476**, 105 (2011).

[12] A. N. Boettiger, B. Bintu, J. R. Moffitt, S. Wang, B. J. Beliveau, G. Fudenberg, M. Imakaev, L. A. Mirny, C.-t. Wu, and X. Zhuang, Nature (London) **529**, 418 (2016).

[13] D. Jost, P. Carrivain, G. Cavalli, and C. Vaillant, Nucl. Acids Res. **42**, 9553 (2014).

[14] M. Barbieri, M. Chotalia, J. Fraser, L.-M. Lavitas, J. Dostie, A. Pombo, and M. Nicodemi, Proc. Natl. Acad. Sci. USA **109**, 16173 (2012).

[15] I. B. Dodd, M. A. Micheelsen, K. Sneppen, and G. Thon, Cell **129**, 813 (2007).

[16] K. Sneppen, M. A. Micheelsen, and I. B. Dodd, Mol. Syst. Biol. **4**, 182 (2008).

[17] D. Jost, Phys. Rev. E **89**, 010701(R) (2014).

[18] T. Garel, H. Orland, and E. Orlandini, Eur. Phys. J. B **12**, 261 (1999).

[19] D. Michieletto, E. Orlandini, and D. Marenduzzo, Phys. Rev. X **6**, 041047 (2016).

[20] D. Coli, D. Michieletto, D. Marenduzzo, and E. Orlandini, arXiv:1807.11101.

[21] R. B. Deal, J. G. Henikoff, and S. Henikoff, Science **328**, 1161 (2010).

[22] M. F. Dion, T. Kaplan, M. Kim, S. Buratowski, N. Friedman, and O. J. Rando, Science **315**, 1405 (2007).

[23] D. Michieletto, M. Chiang, D. Colì, A. Papantonis, E. Orlandini, P. R. Cook, and D. Marenduzzo, Nucl. Acids Res. **46**, 83 (2017).

[24] P. G. de Gennes, J. Phys. Lett. **36**, 55 (1975).

[25] M. A. Moore, J. Phys. A **10**, 305 (1977).

[26] I. M. Lifshitz, A. Y. Grosberg, and A. R. Khokhlov, Rev. Mod. Phys. **50**, 683 (1978).

[27] J. R. Dixon, S. Selvaraj, F. Yue, A. Kim, Y. Li, Y. Shen, M. Hu, J. S. Liu, and B. Ren, Nature (London) **485**, 376 (2012).

[28] See Supplemental Material at http://link.aps.org/supplemental/10.1103/PhysRevE.100.060401 for derivations and detailed analysis.

[29] M. Doi and S. F. Edwards, *The Theory of Polymer Dynamics* (Clarendon, Oxford, 1986).

[30] P. G. de Gennes, *Scaling Concepts in Polymer Physics* (Cornell University Press, Ithaca, NY, 1979).

[31] K. Yoshikawa, M. Takahashi, V. V. Vasilevskaya, and A. R. Khokhlov, Phys. Rev. Lett. **76**, 3029 (1996).

[32] A. Zinchenko, N. V. Berezhnoy, S. Wang, W. M. Rosencrans, N. Korolev, J. R. C. van der Maarel, and L. Nordenskiöld, Nucl. Acids Res. **46**, 635 (2017).

[33] F. Y. Wu, Rev. Mod. Phys. **54**, 235 (1982).

[34] J.-H. Huang and M.-B. Luo, Polymer **45**, 2863 (2004).

[35] P.-Y. Lai, Physica A **221**, 233 (1995).

[36] A. Halperin and E. B. Zhulina, Europhys. Lett. **15**, 417 (1991).

[37] P. Grassberger and H.-P. Hsu, Phys. Rev. E **65**, 031807 (2002).

[38] P. L. Geissler and E. I. Shakhnovich, Phys. Rev. E **65**, 056110 (2002).

[39] D. Michieletto, E. Orlandini, and D. Marenduzzo, Sci. Rep. **7**, 14642 (2017).

[40] J. Sima, A. Chakraborty, V. Dileep, M. Michalski, K. N. Klein, N. P. Holcomb, J. L. Turner, M. T. Paulsen, J. C. Rivera-Mulia, C. Trevilla-Garcia, D. A. Bartlett, P. A. Zhao, B. K. Washburn, E. P. Nora, K. Kraft, S. Mundlos, B. G. Bruneau, M. Ljungman, P. Fraser, F. Ay, and D. M. Gilbert, Cell **176**, 816 (2019).

[41] A. R. Strom, A. V. Emelyanov, M. Mir, D. V. Fyodorov, X. Darzacq, and G. H. Karpen, Nature (London) **547**, 241 (2017).

[42] A. G. Larson, D. Elnatan, M. M. Keenen, M. J. Trnka, J. B. Johnston, A. L. Burlingame, D. A. Agard, S. Redding, and G. J. Narlikar, Nature (London) **547**, 236 (2017).

[43] A. J. Plys, C. P. Davis, J. Kim, G. Rizki, M. M. Keenen, S. K. Marr, and R. E. Kingston, bioRxiv, 467316 (2018).

[44] R. Tatavosian, S. Kent, K. Brown, T. Yao, H. N. Duc, T. N. Huynh, C. Y. Zhen, B. Ma, H. Wang, and X. Ren, J. Biol. Chem. **294**, 1451 (2019).

[45] M. J. Obersriebnig, E. M. H. Pallesen, K. Sneppen, A. Trusina, and G. Thon, Nat. Commun. **7**, 11518 (2016).